Cubic Hermite Interpolations of Signed Distance Fields

Viktor A. Vad Eötvös Loránd University Pázmány P. stny 1/C. Hungary 1117, Budapest vad@inf.elte.hu Gábor Valasek Eötvös Loránd University Pázmány P. stny 1/C. Hungary 1117, Budapest valasek@inf.elte.hu

Abstract

Signed distances are frequently employed concepts in computer graphics and geometric modeling. In high-performance applications, these are most often approximated by bilinearly filtered regular grids of signed distance samples. However, this framework does not preserve the fundamental properties and behavior of signed distance functions, such as unit length gradients and the recently proposed null closest point energies. Hermite interpolation, in particular its cubic realization, has been well established in the domain of signal processing. Although these have been also shown to be efficient means to approximate signed distance functions from a general loss perspective, their relation to these properties have not been investigated previously. We present a comparative empirical study on various Hermite interpolation constructs focusing on how the resulting approximants deviate from the properties of true signed distance functions.

Keywords

Computer Graphics, interpolation, Signed Distance, Hermite interpolation

1 INTRODUCTION

Signed distance functions (SDFs) are essential in computer graphics and geometric modeling. In real-time graphics, SDFs are evaluated on discrete samples arranged in a regular grid, and during rendering, a reconstructed function approximates the unknown original.

Most often the fast and simple built-in bilinear filtering is used for the reconstruction. However, recent advancements have proposed higher-order reconstruction methods for SDFs.

These existing methods focus on minimizing the error between the original and reconstructed SDF. Yet, evaluating the quality of an approximation to an SDF requires the consideration of additional properties. In some applications, e.g., visualization [Har96, BBV19], maintaining an SDF-like structure is more critical than achieving perfect reconstruction accuracy.

Recently, Marschner et al. pointed out [MSLJ23], that simple unit gradient length constraints are insufficient to guarantee SDF properties. They proposed closest point energy as a new metric to measure SDF fidelity.

Permission to make digital or hard copies of all or part of this work for personal or classroom use is granted without fee provided that copies are not made or distributed for profit or commercial advantage and that copies bear this notice and the full citation on the first page. To copy otherwise, or republish, to post on servers or to redistribute to lists, requires prior specific permission and/or a fee. In this paper, we review methods based on cubic Hermite interpolation from an SDF reconstruction perspective. While it is evident that algebraic surfaces, such as Hermite cubics, cannot possess unit length gradients, the extent to which they can approximate other SDF properties is not a well studied area.

Our experiments were conducted in 2D for ease of reproduction, though the approach can be extended to any dimension, particularly 3D.

The paper is organized as follows. Section 2 provides an overview of SDF reconstruction methods, with particular focus on Hermite interpolation approaches. In Section 3, we present the computation of analytic SDF derivatives and introduce our solution to a key practical issue. Section 4 details the Hermite interpolation methods under investigation, while Section 5 presents and discusses our experimental findings.

2 RELATED WORK

General reconstruction of SDFs

A discrete signed distance representation consist of two components: i) a finite set of data and ii) an algorithm that combines the data into an analytic functional approximation to the original SDF. The latter is most often referred to as filtering or interpolation.

Perhaps the most straightforward realization of this concept is a regular grid of SDF samples that are combined by bilinear interpolation. This approach gained popularity in anti-aliased font rendering applications following Green's publication [Gre07]. They

proposed to use 2D textures to represent the signed distance field. Each texel stores its signed distance to the closest boundary curve of a glyph, i.e., a character in the font. Bilinear interpolation of these values yields a C^0 approximation to the SDF of each glyph. The interpolated distance is used for anti-aliasing and other distance-based effects. Here, the versatility of the distance representation is paired with efficient queries via hardware accelerated bilinear texture filtering.

Despite these advantages, a practical observation is also often raised as a drawback of SDF textures: they tend to round out sharp features, unless a high resolution grid is used. While the phenomenon is indeed apparent, it is usually incorrectly attributed entirely to SDF textures themselves, whereas it is equally caused by the way the samples are interpreted and combined.

A new approach was taken by Chlumsky et al.[CSv18] where a multi-channel formulation was presented to alleviate the smoothing observed in bilinearly filtered SDFs. The single distance value is replaced by three pseudo-distances at each texel that denote the pseudo-SDF values for shapes bounded by subsets of the original boundary curves. Upon query, the median of these values is used.

An alternative to preserve sharp features is to increase the descriptive power of a sample itself. Koschier et al. [KDB16] proposed to use independent local polynomial approximations to the SDF over disjoint regions of space. The distance approximation is the result of the evaluation of the closest polynomial using the coordinates of the query position.

Hermite-based reconstructions

Valasek and Bán [VB23] proposed an approach where polynomial approximations are combined such that the resulting approximation is globally continuous up to a higher order. One of their solutions was to store SDF values and partial derivatives at the samples and use Hermite interpolation to obtain a tri-cubic polynomial that reconstructs the SDF values and gradients exactly at the vertices. Since this is an underdetermined problem, they set the first mixed partial derivatives to obtain the volume version of the Ferguson patch. They referred to this as Ferguson-Hermite interpolation. This approach was latter shown to be compatible with adaptive spatial subdivision [BV23] and extended to use the generalization of the Adini-twist to volumes to infer a better mixed partial derivative estimate [BV25].

Song et al. formulated the SDF reconstruction as a general function approximation problem and used polynomial splines over hierarchical T-meshes as approximants [SJP10]. These were demonstrated on reconstructing first order data, that is, values and gradients. The derivatives were computed from the parametric form of the input.

Our paper investigates how Hermite interpolation is applied to the approximation of SDFs. Prior work focused on different heuristics and mechanics to obtain SDF derivative data. We compare these to inspect how well the resulting polynomial approximations preserve the SDF property of the input.

This is often derived from how far away from an Eikonal the approximant is, that is, how much its gradient deviates from being unit length. However, Marschner et al. [MSLJ23] showed that even if a field is changed to conform to this constraint, it still does not necessarily yield an actual SDF. Instead, they proposed the incorporation of the closest point energy to the formulations to encourage the optimization of neural implicits to form a true distance function.

Hermite interpolation requires partial derivative data in addition to the SDF values. These gradient values can be either computed analytically or estimated from samples. In this work, we investigate methods of both of these approaches.

3 ANALYTIC DERIVATIVES OF SDF

The $c \in \mathbb{R}$ level set of an $f : \mathbb{E}^2 \to \mathbb{R}$ implicit function is written as $\{f = c\} = \{\mathbf{x} \in \mathbb{E}^2 \mid f(\mathbf{x}) = c\}$. Similarly, $\{f \le c\} = \{\mathbf{x} \in \mathbb{R}^2 \mid f(\mathbf{x}) \le c\}$. An $f : \mathbb{R}^2 \to \mathbb{R}$ function is a *distance function* (DF) if

$$f(\mathbf{x}) = d(\mathbf{x}, \{f = 0\}) = \inf\{\|\mathbf{x} - \mathbf{y}\| \mid f(\mathbf{y}) = 0\},\$$

and a *signed distance function* (SDF) if it is continuous and |f| is a distance function [BVG19]. In case of a $\mathbf{c} : [a,b] \to \mathbb{E}^2$ parametric curve, the DF is defined as

$$f(\mathbf{x}) = \inf\{\|\mathbf{x} - \mathbf{y}\| \mid \exists t \in [a, b] : \mathbf{c}(t) = \mathbf{y}\},$$
 (2)

and the SDF is analogous to the implicit case. While the concept itself is elegant, in practice, a closed-form realization of the SDF of a free-form shape is just as an elusive artifact as the arc-length parametrization of integral and rational polynomial curves. However, its analytical properties are surprisingly tangible.

Song et al. [SJP10] derived a formula for computing the mixed partial derivatives of an SDF function. Their approach assumes the existence of a footparameter mapping $t: \mathbb{E}^2 \to [a,b]$, which computes the \boldsymbol{p} closest point on the curve to a given \boldsymbol{x} query position as $\boldsymbol{p} = \boldsymbol{c}(t(\boldsymbol{x}))$. We refer to the closest curve point as a footpoint.

The gradient of an f SDF of c(s) can be written as

$$\nabla f(\mathbf{x}) = \pm \frac{\mathbf{x} - \mathbf{c}(t(\mathbf{x}))}{\|\mathbf{x} - \mathbf{c}(t(\mathbf{x}))\|} . \tag{3}$$

The second order derivatives of the SDF require ∇t . However, the authors showed that ∇t could be estimated by solving a linear system.

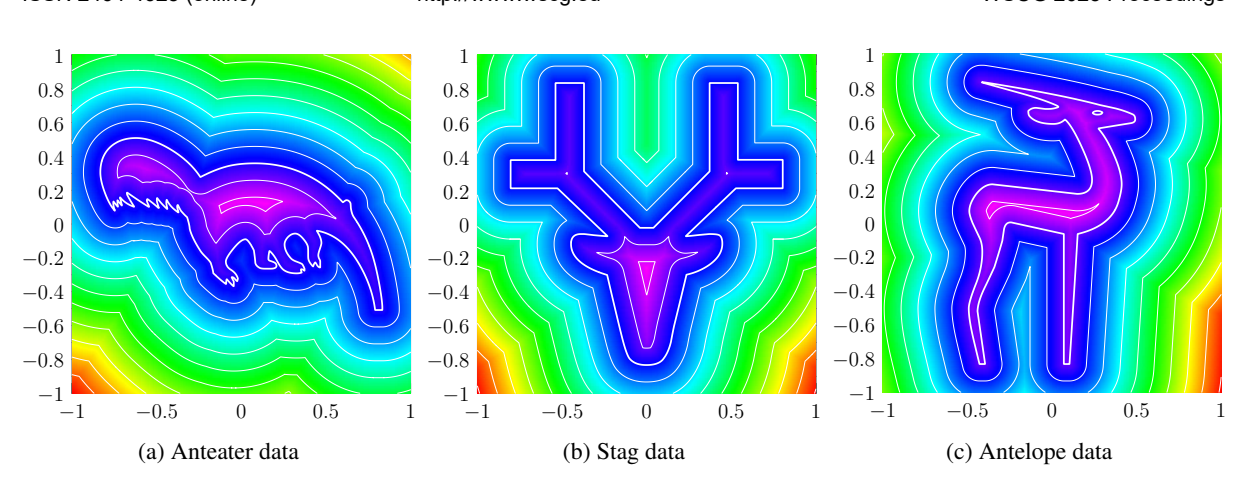


Figure 1: SDF data used for measurements.

A practical issue arises with the formalism above: the gradient includes the reciprocal of the distance between the footpoint and the query position, a term that also appears in the second-order gradient expression. This becomes a concern when a sample position approaches the curve, as numerical instabilities arise. Despite the SDF being smooth – even on the curve itself – nearby samples produce incorrect second-order gradient values due to division by diminishing distances.

To address this, we leverage that the gradient of a 2D SDF is always perpendicular to the tangent of the curve at the footpoint, that is,

$$(\boldsymbol{x} - \boldsymbol{c}(t(\boldsymbol{x})))^T \cdot \boldsymbol{c}'(t(\boldsymbol{x})) = 0,$$

holds if the curve is twice differentiable at the footpoint. In this case, the gradient of the SDF is obtained by rotating the $c'(t(\mathbf{x}))$ curve tangent at the footpoint by a $\pm 90^{\circ}$ rotation and normalization. This approach eliminates the distance term from ∇f , with the rotation sign determined by the winding order of the curve. However, this solution is only valid when the footpoint lies on a smooth curve segment. For non-smooth regions, particularly at corners, the original formulation is used.

4 METHODOLOGY

Hermite Interpolation

Assume that a grid on plane is defined by points $[x_i, y_j] \in \mathbb{R}^2$, where $i, j \in \mathbb{Z}$, $x_i = i * \Delta x, y_j = j * \Delta y$, Δx , Δy are the distance of the grid points in x and y direction respectively. Then 2D Hermite Spline is defined as

$$H(x,y) = \sum_{k,l=0}^{1} (c_{i+k,j+l}h_{0,k}(s)h_{0,l}(t) + g_{i+k,j+l}^{x}h_{1,k}(s)h_{0,l}(t)\Delta x + (4) g_{i+k,j+l}^{y}h_{0,k}(s)h_{1,l}(t)\Delta y + g_{i+k,j+l}^{xy}h_{1,k}(s)h_{1,l}(t)\Delta y\Delta x),$$

where h_{ij} are the Cubic Hermite basis functions[Ska22], $x \in [x_i, x_{i+1}], y \in [y_j, y_{j+1}]$ for some $i, j \in \mathbb{Z}$, and $s, t \in [0, 1]$ are the local basis coordinates, such that $x = x_i + s\Delta x$ and $y = y_j + t\Delta y$.

If $f: \mathbb{R}^2 \to \mathbb{R}$ is twice differentiable at grid points, setting $c_{i,j} = f(x_i, y_j)$, $g_{i,j}^z = \partial_z f(x_i, y_j)$, $z \in \{x, y\}$ and $g_{i,j}^{xy} = \partial_{xy} f(x_i, y_j)$ yields (4) to interpolate f up to first order and cross partial derivatives.

In practice, since the analytic gradient coefficients (exact derivatives) are often unknown, they are typically estimated using numerical methods. We are investigating some of these methods used for SDF interpolation.

Least-squares fitting based gradient estimations

Most of the methods that are investigated in this work assumes that gradient of SDF is known, and only cross partial derivative needs to be estimated numerically. To ensure fair comparisons and to establish a consistent baseline, we computed Hermite derivative coefficients using linear least squares fitting (LSQ).

Rather than solving one large linear system to compute all the missing coefficients in Equation (4), decomposed the problem into three tractable sub-problems. At the grid points where Equation (4) is evaluated, only the weights associated with $c_{i,j}$ are non-zero, and these weights are equal to one. Hence, $c_{i,j} = f(x_i, y_j)$. Next, we placed sample positions along the edges of grid cells, initially in the x-direction. When evaluating Equation (4) at these positions, only $c_{i,j}$ (already known) and $g_{i,j}^x$ contribute with non-zero weights. We sampled 16 positions from the SDF on each edge aligned in the x-direction and estimated the $g_{i,j}^x$ coefficients by solving a much smaller linear system. The same procedure was then applied in the y-direction.

At this point, the only remaining unknowns were the cross-derivative coefficients $g_{i,j}^{xy}$, which we estimated using 16×16 interior samples per grid cell.

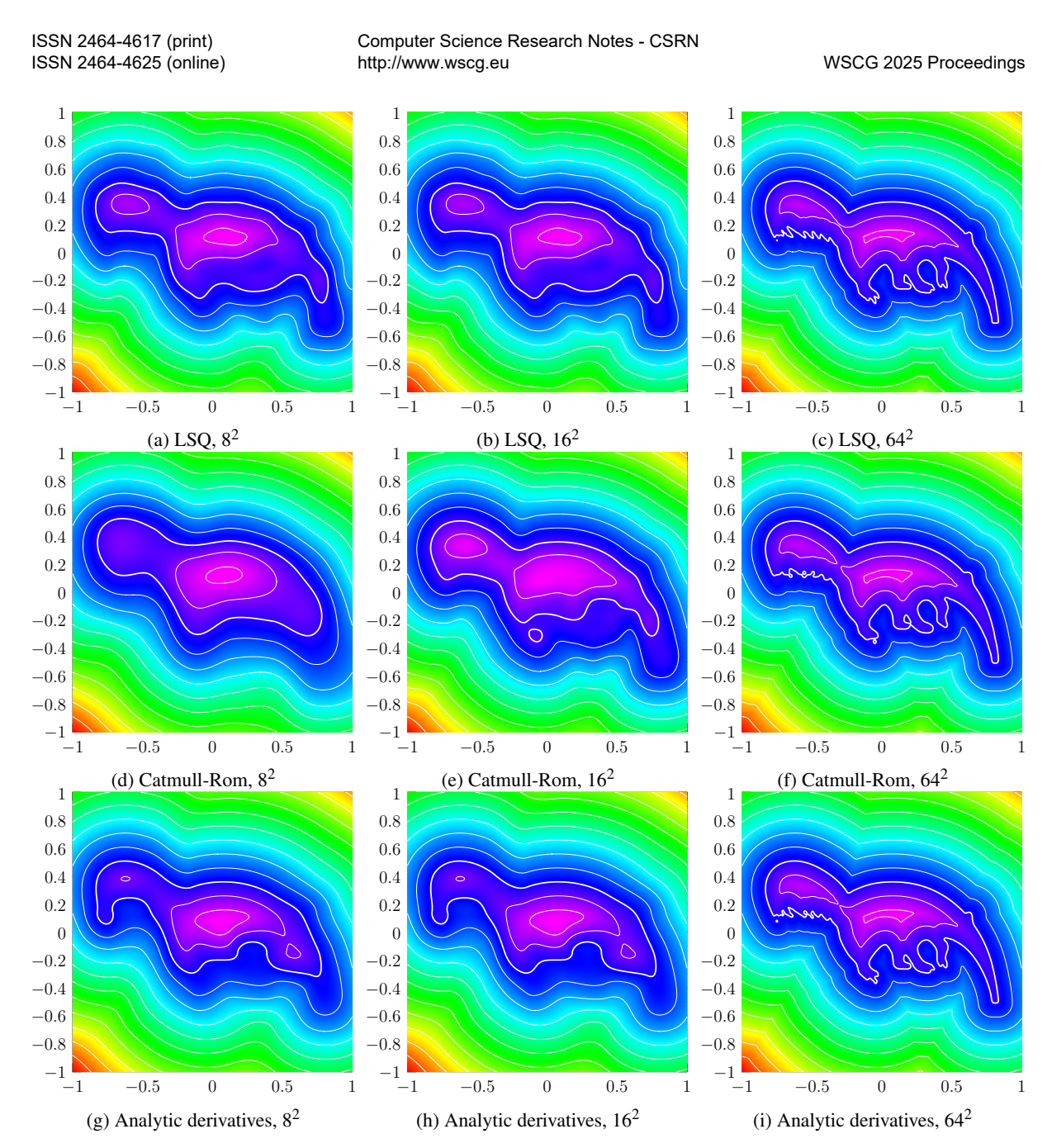


Figure 2: SDF reconstructions of anteater data

We assume that LSQ-based Hermite reconstruction represents the best possible outcome for cubic Hermite interpolation from a function reconstruction perspective. As shown later, our results support this assumption.

Investigated Hermite methods

We examined cubic Hermite methods that have been previously used for SDF reconstruction. These primarily differ in how gradients($g_{i,j}^x$, $g_{i,j}^y$) and mixed derivatives ($g_{i,j}^{xy}$) are estimated.

The classic approach approximates gradients using central differences and derives mixed partial derivatives from these first-order estimates. This corresponds to a special case of Catmull-Rom spline surfaces.

Song et al. [SJP10] proposed an analytical formulation for computing both gradients and mixed derivatives. While we included test cases with their analytical derivatives, we substituted them with our numerically stable formulation where applicable.

Valasek and Bán [VB23] introduced a reconstruction method based on resampling a Ferguson patch. For cubic Hermite patches, this is equivalent to assuming vanishing mixed gradients. In our experiments, we computed directional gradients analytically and explicitly set mixed partials to zero.

The same authors also proposed estimating Hermite algebraic derivatives (HAD) via local least-squares fitting. We adopted this method exclusively for mixed

		Catmull-Rom	LSQ	Analitic derivatives	Ferguson	Adini twist	HAD
	4	0.056	0.028	0.036	0.036	0.034	0.039
RMS	8	0.024	0.013	0.023	0.023	0.023	0.017
	16	0.009	0.003	0.006	0.006	0.006	0.006
	32	0.003	0.001	0.002	0.002	0.002	0.002
	64	0.001	0.000	0.001	0.001	0.001	0.001
	4	0.566	0.751	0.717	0.717	0.732	0.684
	8	0.788	0.840	0.784	0.777	0.777	0.808
IoU	16	0.871	0.957	0.926	0.924	0.924	0.912
	32	0.962	0.979	0.975	0.976	0.976	0.973
	64	0.985	0.994	0.992	0.992	0.992	0.991
	4	0.367	0.300	0.265	0.269	0.268	0.322
	8	0.240	0.213	0.206	0.203	0.203	0.220
Length Deviation	16	0.211	0.154	0.166	0.166	0.166	0.175
-	32	0.147	0.115	0.118	0.118	0.118	0.126
	64	0.105	0.081	0.086	0.086	0.086	0.090
	4	37.186	30.924	36.800	36.521	34.955	34.235
	8	29.073	23.697	30.541	30.888	30.836	24.991
Angular Deviation	16	21.497	13.387	16.600	16.628	16.621	15.537
_	32	14.174	9.553	12.061	11.878	11.876	11.087
	64	9.886	5.990	8.071	8.095	8.095	7.325
	4	0.061	0.046	0.043	0.044	0.044	0.048
	8	0.042	0.027	0.028	0.028	0.028	0.034
CPE (original gradients)	16	0.022	0.014	0.016	0.016	0.016	0.016
	32	0.012	0.008	0.007	0.007	0.007	0.009
	64	0.006	0.004	0.004	0.004	0.004	0.004
	4	0.053	0.031	0.034	0.034	0.033	0.042
	8	0.029	0.018	0.019	0.019	0.019	0.024
CPE (normalized gradients)	16	0.015	0.009	0.011	0.011	0.011	0.010
	32	0.007	0.004	0.004	0.004	0.004	0.005
	64	0.003	0.002	0.002	0.002	0.002	0.003

Table 1: Measured errors for the **anteater** data. Angular deviation is meant in degrees.

		Catmull-Rom	LSQ	Analitic derivatives	Fergusson	Adini twist	HAD
	4	0.092	0.039	0.071	0.073	0.072	0.059
RMS	8	0.032	0.012	0.018	0.018	0.018	0.019
	16	0.010	0.003	0.006	0.006	0.006	0.006
	32	0.003	0.001	0.002	0.002	0.002	0.002
	64	0.001	0.000	0.001	0.001	0.001	0.001
	4	0.140	0.712	0.488	0.475	0.449	0.398
	8	0.699	0.884	0.849	0.845	0.843	0.826
IoU	16	0.917	0.976	0.972	0.972	0.972	0.963
	32	0.986	0.993	0.994	0.994	0.994	0.993
	64	0.996	0.999	0.998	0.998	0.998	0.998
	4	0.566	0.370	0.420	0.424	0.427	0.473
	8	0.362	0.269	0.276	0.280	0.279	0.300
Length Deviation	16	0.247	0.177	0.192	0.193	0.193	0.199
	32	0.180	0.131	0.139	0.138	0.138	0.143
	64	0.119	0.087	0.094	0.094	0.094	0.098
	4	62.449	39.514	46.593	46.711	48.275	40.040
	8	34.765	21.209	28.903	28.334	28.517	25.702
Angular Deviation	16	20.955	11.640	15.940	15.934	15.881	14.235
	32	13.358	7.497	10.919	10.883	10.878	9.469
	64	9.672	5.703	8.039	8.041	8.040	6.955
	4	0.076	0.056	0.058	0.059	0.055	0.053
	8	0.049	0.036	0.033	0.034	0.033	0.036
CPE (original gradients)	16	0.027	0.017	0.018	0.019	0.019	0.019
	32	0.015	0.010	0.009	0.009	0.009	0.010
	64	0.008	0.005	0.004	0.005	0.005	0.005
	4	0.066	0.035	0.046	0.048	0.042	0.044
	8	0.027	0.017	0.016	0.017	0.017	0.019
CPE (normalized gradients)	16	0.014	0.007	0.009	0.009	0.009	0.010
	32	0.007	0.003	0.004	0.004	0.004	0.004
	64	0.003	0.001	0.002	0.002	0.002	0.002

Table 2: Measured errors for the **stag** data. Angular deviation is meant in degrees.

derivatives, following their suggested approach: for each texel, we sampled the SDF on a fine 7^2 grid (covering the dual of the input grid) and fitted a polynomial to the samples.

Additionally, the authors generalized the Adini twist technique to volumes [BV25]. For our experiments, however, we retained the original surface patch for-

mulation. This means that for each sample located at the corner of four cells, we computed a Coons patch [Coo67] using analytical directional derivatives. In our case, the cubic Hermite patch formalism allows closedform estimation of mixed gradients, namely

$$g_{i,j}^{xy} \approx \Delta x (g_{i,j+1}^{x} - g_{i,j-1}^{x}) + \Delta y (g_{i+1,j}^{y} - g_{i-1,j}^{y}) - (c_{i+1,j-1} - c_{i-1,j-1}) - (c_{i+1,j+1} - c_{i-1,j+1}).$$

		Catmull-Rom	LSQ	Analitic derivatives	Ferguson	Adini twist	HAD
	4	0.066	0.037	0.051	0.052	0.052	0.053
RMS	8	0.027	0.010	0.018	0.018	0.018	0.017
	16	0.009	0.004	0.006	0.006	0.006	0.006
	32	0.003	0.001	0.002	0.002	0.002	0.002
	64	0.001	0.000	0.001	0.001	0.001	0.001
	4	0.296	0.468	0.472	0.474	0.460	0.303
	8	0.516	0.807	0.721	0.718	0.720	0.680
IoU	16	0.757	0.926	0.895	0.895	0.895	0.850
	32	0.920	0.969	0.962	0.962	0.962	0.951
	64	0.981	0.990	0.995	0.995	0.995	0.992
	4	0.421	0.413	0.396	0.399	0.394	0.445
	8	0.325	0.258	0.266	0.266	0.265	0.288
Length Deviation	16	0.253	0.190	0.196	0.198	0.197	0.218
_	32	0.180	0.138	0.142	0.142	0.142	0.154
	64	0.127	0.097	0.099	0.099	0.099	0.107
	4	62.576	36.459	41.168	41.972	40.931	55.161
	8	34.999	19.238	26.099	26.156	26.118	25.064
Angular Deviation	16	23.813	12.482	16.941	17.057	17.034	16.632
	32	15.721	7.499	11.239	11.257	11.254	10.096
	64	9.771	5.078	7.599	7.602	7.601	6.555
	4	0.091	0.066	0.075	0.077	0.076	0.078
	8	0.044	0.026	0.032	0.032	0.032	0.035
CPE (original gradients)	16	0.026	0.014	0.015	0.016	0.016	0.018
	32	0.013	0.009	0.008	0.008	0.008	0.009
	64	0.006	0.004	0.003	0.003	0.003	0.004
	4	0.070	0.048	0.061	0.062	0.061	0.065
	8	0.034	0.016	0.023	0.023	0.023	0.026
CPE (normalized gradients)	16	0.018	0.007	0.009	0.010	0.010	0.012
, ,	32	0.008	0.004	0.005	0.005	0.005	0.005
	64	0.003	0.002	0.001	0.002	0.002	0.002

Table 3: Measured errors for the antelope data. Angular deviation is meant in degrees.

		Catmull-Rom	LSQ	Analitic derivatives	Ferguson	Adini twist	HAD
	4	0.845	0.721	1.583	1.417	1.524	0.869
	8	0.660	0.070	0.259	0.359	0.362	0.448
RMS	16	0.145	0.006	0.020	0.043	0.042	0.050
	32	0.012	0.001	0.001	0.004	0.004	0.003
	64	0.001	0.000	0.000	0.000	0.000	0.000

Table 4: Measured RMS errors for function $f(x, y) = \sin(9(x^2 + y^2)) + 3(x + y)$.

Error metrics

We used the root mean square (RMS) deviation metric to quantify the general approximation power of each method.

We adopted the intersection over union (IoU) metric to assess shape preservation capabilities, commonly used in computer vision for comparing binary shape similarity. For IoU measurements, we generated binary images from both the analytic SDF and its Hermite reconstruction, where pixel values indicate interior/exterior membership relative to the shape. This allowed us to quantify shape distortion independent of function approximation errors.

A straightforward way to assess how well the reconstructed function adheres to the Eikonal property is by measuring the deviation of the gradient magnitude from unity. In addition, we measured the angular deviation of the gradients of the SDF and the cubic approximations.

Marschner et al. [MSLJ23] introduced the closest point energy (CPE) metric to improve SDF reconstructions. This method approximates the SDF using gradients at multiple sample points. For each sample, a new position is computed by stepping back along the negative gradient, using the signed distance as the step size. The

absolute reconstructed distances at these new positions are then summed to obtain the CPE.

Originally, CPE was used for training neural pseudo-SDFs, where gradients satisfy the Eikonal property. However, this assumption does not hold for polynomial reconstructions. We therefore also used a modified CPE where gradients are normalized before the backward step. This adaptation allows evaluation of both the accuracy of reconstructed SDF values and the correctness of gradient directions, independent of gradient magnitude deviations, which are inherent in polynomial representations. Our experiments demonstrate that this modified CPE consistently produces lower energy values for polynomial reconstructions compared to the original formulation.

5 RESULTS

We tested each method on three distinct contour datasets, referred to as anteater, stag and antelope. The data comes from FreeType letter contours available online[fon]. Each letter contour is composed of multiple linear and quadratic Bézier curves.

Among the three, the anteater contour is more complex, consisting of hundreds of curves. It features sharp edges, highly variable segments, and smooth contours.

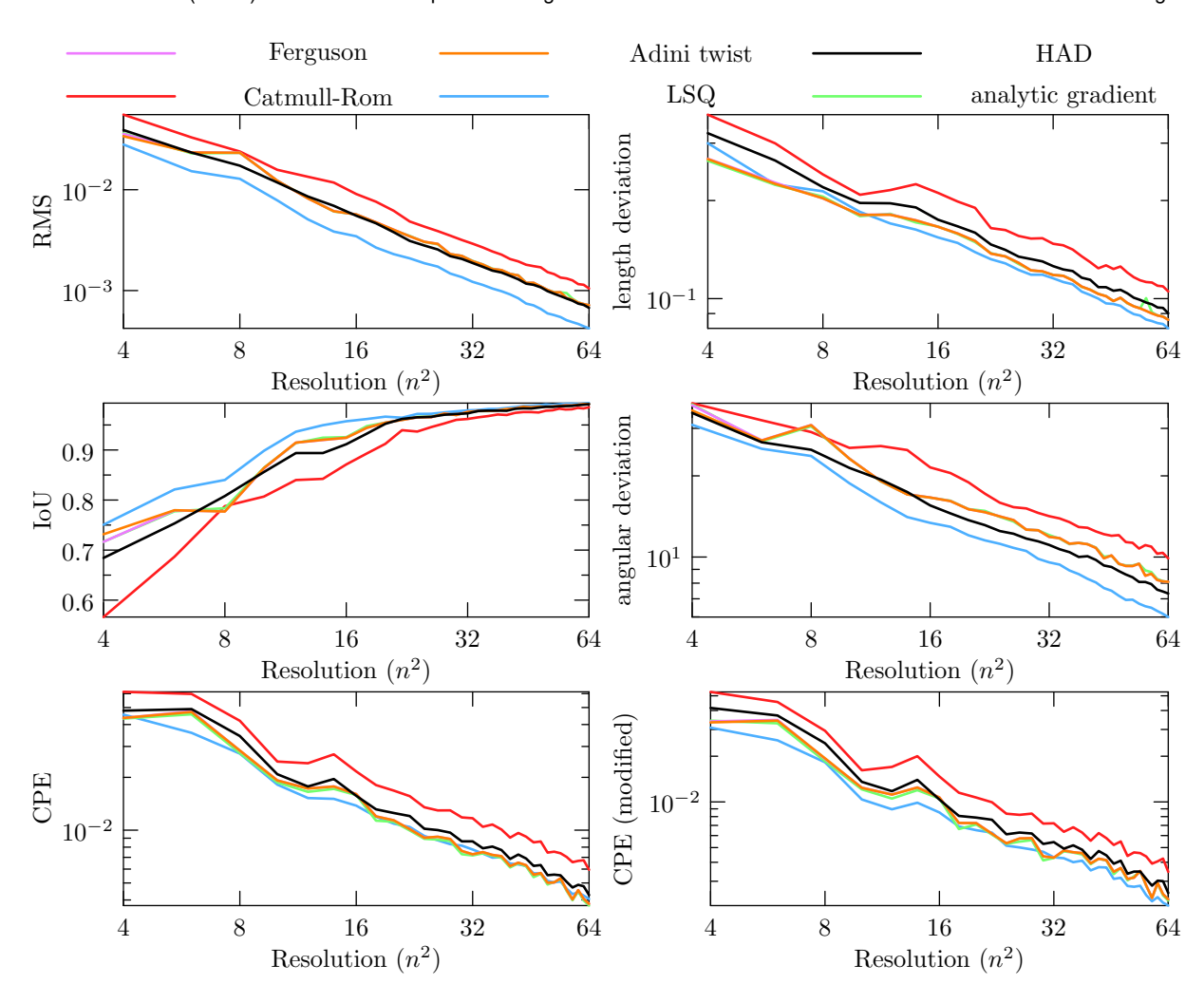


Figure 3: Plots of error metrics used in our measurements, taken from **anteater** data. Generally, plots are in logarithmic scale, and smaller value is better. For IoU, results are plotted linearly, and the higher value is better.

This complex geometry makes it an especially demanding test case for reconstruction quality. Figure 1 shows the analytic representation of these test contours.

We sampled the analytic SDF at progressively finer grid resolutions and reconstructed the SDF using each method. Then, we applied each metric at every resolution. The reconstruction results are shown in Figure 2. The results of our measurements are summarized on Table 1 for the anteater, Table 2 for the stag and Table 3 for the antelope data.

The Catmull-Rom spline method consistently demonstrated the poorest performance across all resolution levels, which was expected given its exclusive reliance on finite-difference gradient approximations rather than analytically computed or high-precision estimated gradients.

The least squares method yielded the best results, which aligns with our assumption since Hermite bases are polynomial. Moreover, LSQ reconstructions exhibit

similar or often superior SDF properties compared to other methods, as evidenced by the angular deviation.

In general, the length deviation error remains significantly high for all methods and resolutions. Although the RMS and IoU metrics indicate adequate reconstructions, the length deviation consistently stays around 0.1 (10% of the reference unit gradient magnitude).

Length deviation also impacts the closest point energy metric. This effect is absent in the modified closest point energy values, which are approximately half of the original measurements. See Figure 4.

Based on these results, while Hermite interpolation accurately approximates the SDF values, it does not preserve the key SDF properties, such as unit-length gradients, gradient directions, or CPE to the same degree.

The methods described above were demonstrated for interpolation of SDFs. However, these methods are general and applicable to any function, they can be used on any function. To illustrate this, we interpolate the function $f(x,y) = \sin(9(x^2 + y^2)) + 3(x + y)$. Since this

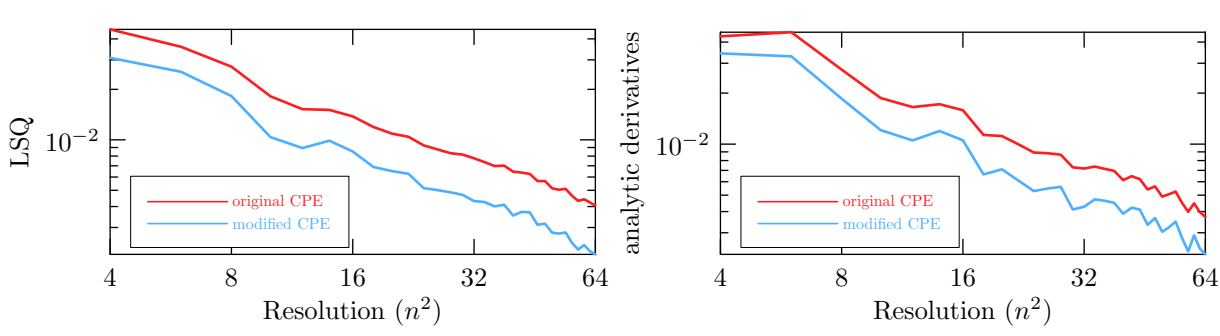


Figure 4: Comparing original CPE and modified CPE for LSQ gradients and analytic gradients. Axes are in log scale. Modified CPE values are approximately half of the original measurements.

is not a distance field, SDF-specific metrics are not applicable; thus, we report only RMS errors for all gradient estimation methods. Measurement results can be found on Table 4.

6 CONCLUSIONS

We investigated cubic Hermite interpolation based reconstruction of signed distance functions. Beyond the standard root mean square error, we also investigated how similar to an SDF the approximants are.

We incorporated the recently proposed metric tailored for pseudo SDFs. We proposed a modification which diminishes the necessity of Eikonal property.

Empirically, we demonstrated that the best results are obtained by least squares fitting. However, all methods suffer from non-unit gradient magnitudes, that is a necessary condition for SDFs.

As future work, we plan to investigate how the findings from this study can be incorporated into gradient fitting and estimation methods for cubic Hermite reconstruction of signed distance functions.

7 REFERENCES

- [BBV19] Róbert Bán, Csaba Bálint, and Gábor Valasek. Area Lights in Signed Distance Function Scenes. In Paolo Cignoni and Eder Miguel, editors, *Eurographics 2019 Short Papers*. The Eurographics Association, 2019.
- [BV23] Róbert Bán and Gábor Valasek. Sparse Ferguson-Hermite Signed Distance Fields. In Gurprit Singh and Mengyu (Rachel) Chu, editors, *Eurographics 2023 Posters*. The Eurographics Association, 2023.
- [BV25] Róbert Bán and Gábor Valasek. Hermite interpolation of scalar fields in computer graphics. *Computer-Aided Design and Applications*, 22(5):927–946, 2025.
- [BVG19] Csaba Bálint, Gábor Valasek, and Lajos Gergó. Operations on Signed Distance Functions. *Acta Cybernetica*, 24(1):17–28, May 2019.

- [Coo67] S. A. Coons. Surfaces for computer-aided design of space forms. Technical report, Massachusetts Institute of Technology, USA, 1967.
- [CSv18] V. Chlumský, J. Sloup, and I. Šimeček. Improved corners with multi-channel signed distance fields. *Computer Graphics Forum*, 37(1):273–287, 2018.
- [fon] WM Animals 2 Font FONT Repo Free TTF Fonts fontrepo.com. https://www.fontrepo.com/font/17449/wmanimals2. [Accessed 22-04-2025].
- [Gre07] Chris Green. Improved alpha-tested magnification for vector textures and special effects. In *ACM SIGGRAPH 2007 Courses*, SIGGRAPH '07, page 9–18, New York, NY, USA, 2007. Association for Computing Machinery.
- [Har96] J. Hart. Sphere tracing: a geometric method for the anti aliased ray tracing of implicit surfaces. *The Visual Computer*, (12):527–545, 1996.
- [KDB16] Dan Koschier, Crispin Deul, and Jan Bender. Hierarchical hp-adaptive signed distance fields. In *Proceedings of the 2016 ACM SIGGRAPH/Eurographics Symposium on Computer Animation*. Eurographics Association, 2016.
- [MSLJ23] Zoë Marschner, Silvia Sellán, Hsueh-Ti Derek Liu, and Alec Jacobson. Constructive solid geometry on neural signed distance fields. In *SIGGRAPH Asia 2023 Conference Papers*, SA '23, New York, NY, USA, 2023. Association for Computing Machinery.
- [SJP10] X. Song, B. Jüttler, and A. Poteaux. Hierarchical spline approximation of the signed distance function. In 2010 Shape Modeling International Conference, pages 241–245, June 2010.
- [Ska22] Vaclav Skala. Hermite parametric bicu-

bic patch defined by the tensor product. In Computational Science and Its Applications – ICCSA 2022: 22nd International Conference, Malaga, Spain, July 4–7, 2022, Proceedings, Part II, pages 228–235. Springer Nature, jul 2022.

[VB23] Gábor Valasek and Rábert Bán. Higher Order Algebraic Signed Distance Fields. *Computer-Aided Design and Applications*, 20(5):1005–1028, 2023. Computer Science Research Notes - CSRN http://www.wscg.eu

ISSN 2464-4617 (print) ISSN 2464-4625 (online)

WSCG 2025 Proceedings